

Chapter 1

1

Chapter 2

Tower Support Structure Design

2.1 Abstract

This study examines two possible alterations to the detector towers for the SuperCDMS Experiment. The first modification involves alternate support tube materials to act as thermal isolators for separate tower stages. Candidates are chosen for low thermal conductivity, low radioactivity, and high strength. The thermal conductivity of Vespel SCP-5000, Vespel SCP-5050, Ti 15-3-3-3, and Ti21S are measured. The gamma radioactivity of all samples were measured. The radius and thickness of the tubes were then optimized to minimize radioactivity and thermal power loading to each stage. The second design alteration proposes low inductance parallel-strip transmission lines to replace current vacuum coaxial wires on the tower face. The thermal loads and inductance calculations are presented.

2.2 Introduction

The CDMS (Cryogenic Dark Matter Search) Experiments

- search for dark matter CDMS in general
- detector operation, limited cooling power, limiting thermal conductivity, limiting radioactivity.

2.3 Tower Support Tube Design

We are proposing design alterations for SNOlab, considering possible alternate materials and dimensions for the central support tubes.

Considerations for Material Candidates:

- Thermal Conductivity
- Radioactivity
- Mechanical Properties

2.3.1 Thermal Conductivity

Due to the finite cooling power of our helium dilution refrigerator, we must limit the thermal load to each stage of the fridge. The tower support tubes are a major source of thermal loading on each stage. The thermal power load on each stage from the tubes is governed by the general equation

$$Power = \int_{T_{low}}^{T_{high}} \frac{A}{L} K(T) dT \quad , \quad (2.1)$$

where T_{low} is the temperature of the stage being loaded, T_{high} is the warmer connecting stage, A is the tube cross-sectional area, L is tube length, and $K(T)$ is the thermal conductivity. From the equation, we can see that thermal power is directly proportional to thermal conductivity, so by decreasing thermal conductivity, we decrease power to each stage. Figure 1 displays the thermal conductivity for tower tube candidate materials.

From the graph, one can see that Ti 15-3-3-3 potentially has a much lower thermal conductivity for the temperature range of the lowest support tube, 100mK to 40mK. Current data only extends down to 230mK, however. At that temperature, it is crossing the lowest thermally conductive material, Vespel SP-22, and decreasing quickly.

Table 1 summarizes the possible improvements in thermal power conducted for each stage, assuming identical tube dimensions.

Next Steps

Implement thermal conductivity tests during tower runs to increase data sets, and verify current data. Build 3He cooler fridge.

2.3.2 Radioactivity

Due to the sensitivity of our detectors, radioactive contamination in our tower materials is a concern, and therefore a consideration when choosing a candidate. Material samples were sent to a test facility to be screened for radioactivity. The results are presented in Table 2, which gives the total activity for nuclear transmutational processes (e.g. α -decay, β -decay, Spontaneous Fission).

Measurement Process

The measurement process used a high purity Ge detector as a gamma counter to measure the gamma decay spectrum of each sample. From this, characteristic lines were identified for the U-238, Th-232, Co-60, K-40 and Cs-137 chains. A Monte Carlo simulation was then performed for each isotope in the chains of interest. This subtracted off background activity and estimated the efficiency of gamma detection for each line, which includes sample geometry and gamma production rate for transmutational decay processes. The result of this simulation was the total activity for each isotope.

Due to the long half-lives of the parent isotopes, the decay chains are assumed to be in secular equilibrium, implying that the decay rates of all isotopes are equal. Due to the finite accuracy of statistics, the activity of the lines were not all equal, so a weighted average of the best lines was taken to then obtain the activity of the parent isotope reported in Table 2.

POCO is dirty because it is industrial grade

Using SOURCES-4C to Predict Neutron Emission Rates

Neutron background is the largest concern for our detectors as it produces a nuclear recoil which, along with no charge collection, mimics the expected signal from WIMPS. In our candidate materials, there are two sources of neutrons: Spontaneous Fission and (α ,n)-reactions. These occur at different rates for

each material, depending on the radioactive decay chain present and its constituent materials, which are the target materials for the (α ,n)-reactions. Therefore, the total activity for each material is not the determining factor; Instead, we must select materials based on acceptable neutron emission rates.

To model the neutron emission rate of each material, we used SOURCES-4C, a program developed by Los Alamos National Laboratory and Texas A&M University. This program allows calculation of neutron emission rates through both spontaneous fission and (α ,n)-reactions using an extensive library of parameters such as reaction and stopping cross-sections, product nuclide level branching fractions, etc.

For our problem, the input parameters for SOURCES-4C were:

1. Constituent elements in atom fraction
2. Alpha sources in atoms/cc
3. Target materials in atom fraction

To determine the α -source contamination in atoms/cc we had to convert from the total activity values in Table 2. We use the equation

$$D = -\frac{R\rho h}{\ln \frac{1}{2}},$$

to find the number of atoms/cc for a given isotope, where R is activity in Becquerels/kg, ρ is the material density in kg/cc, and h is the half-life of the isotope in seconds.

Once we have the contamination of the parent isotope, we can then find the corresponding contamination for all α -emitting daughters using the relation

$$D_d = D_p \frac{h_d}{h_p},$$

where the subscripts d and p represent daughter and parent, respectively.

As seen in Table 3, the neutron emission levels over the duration of an experiment are very low, thus probability of neutron emission is unlikely. For the POCO graphite grades, purification is an option as ACF-10Q, AXM-5Q, and ZXF-5Q are all industrial grades, so have higher impurity levels. Both POCO and Mersen offer purification processes which are able to reduce impurities to <5ppm. These processes place the sample in an environment of chlorine gas pressurized above 15 psi and heated to roughly 2000°C. The chlorine then readily bonds with oxidizable metals to remove them. The POCO samples will be purified and re-screened to test for a reduction in activity levels and the possibility of using them in the tower.

2.3.3 Mechanical Properties

The mechanical properties of the materials determine how little of the material we can safely use, thus setting the total radioactivity and thermal power conducted. Data for our materials was obtained from Matweb, DuPont data sheets, and correspondence with Mersen, the producer of our current graphite, formally known as Grade UF-4S. Relevant properties are presented in Table 3.

- CDMS Graphite has a lower strength than every other material, including AXM-5Q, another graphite.
- The Ti alloys offer high strength and low CTE. Ti 21S will be discussed in Availability section.
- Vespel SCP-5000 is the newly developed replacement for Vespel SP-1 with better mechanical properties and a lower CTE. In the above table, the CTE of Vespel SP-1 is $45\mu\text{m}/\text{mC}$ from 300K to cryogenic temperatures. For temperatures above 300K, its CTE is $54\mu\text{m}/\text{mC}$. The CTE of SCP-5000, $45\mu\text{m}/\text{mC}$, is given for temperatures above 300K. The cryogenic CTE is not known, but would likely be lower than its room temperature value as with Vespel SP-1.

Thermal Contraction

To prevent individual temperature stages from thermally shorting to one another, they must not touch at any temperature between 300K and 40mK. In addition, the tower must not shorten enough to allow our NbTi vacuum coax's to sag and short to the casing. The current design has a 0.03 inch (0.0762cm) gap between each stage. Below room temperature, the CTE of SP-1 is $45\mu\text{m}/\text{mC}$. To get total contraction, ΔL :

$$\Delta L = 45 \frac{\mu\text{m}}{\text{mC}} (L_{\text{tube}})(\Delta T)$$

For the longest tower stage, this gives 0.021 inches. Subtracting off the contraction of the copper tower stage (CTE $\approx 10\mu\text{m}/\text{mC}$) gives a total of 0.018 inches contraction. While this leaves the gap open, the new design may consider lengthening the gap slightly to allow a larger buffer.

As for shorting the NbTi wires, a simple model considers the wires under no tension, and any shortening in length is efficiently taken up by the wires (e.g. pulling them toward the casing). We find that the largest deflection for any stage is 0.083 inches. The wires are centered in the vacuum coax, 0.024 inches from the casing. This means we will have way too

much deflection! We need a better model, different material, or new side coax design.

Possible Next Steps

- Radioactivity screening and thermal conductivity test for Ti21S, Vespel SCP-5000, and Vespel SCP-5050
- Carry out strength tests for materials in support tube dimensions and as bulk material.

2.3.4 Dimension Optimization

We are considering the possibility to decrease thickness and/or radius of tower support tubes. This would significantly decrease thermal power conducted and total radioactivity.

Through discussion with Dr. Sanjay Govindjee at UC Berkeley, a model predicting failure loads for different materials/dimensions as well as optimization of Radius/Thickness (a/t) has been developed. The load considered is the same as that used in the graphite tower break test (one end fixed, the other subjected to a transverse shear force).

The most recent model created by Professor Govindjee considers 4 failure modes:

- Shear Instability (Buckling)
- Bending Instability (Buckling)
- Material Failure from Normal Stresses
- Material Failure from Shear Stresses

His full report can be read starting on page **BLANK**. The summary of the failure formulas and their validities follow.

Tube Geometry

The graphite tube tested had nominal dimensions of thickness $t = 0.028\text{in}$, radius $a = 0.986\text{in}$ (to middle surface), and length $L = 1.334\text{in}$.

For theory, the relevant geometric ratios are

$$\frac{a}{t} = 35.2 \quad (2.2)$$

$$\frac{L}{a} = 1.35 \quad (2.3)$$

$$Z = \frac{(1 - \nu^2)^{\frac{1}{2}} L^2}{at} = 61.5 \text{ (for } \nu = 0.3) \quad (2.4)$$

where Z is Donnell's parameter. These values imply that we have a fairly thin shell of intermediate length. For dimension optimization, these values may change.

Shear Instability

The tube may fail due to shear instability. According to Yamaki, this will occur when the maximum shear stress, $\tau_f = P/\pi at$ exceeds critical torsional stress from a purely torsional load,

$$\tau b = \frac{\pi^2 E}{12(1-\nu^2)} (1-\nu^2)^{\frac{3}{8}} a_s \left(\frac{t}{a}\right)^{\frac{5}{4}} \left(\frac{a}{L}\right)^{\frac{1}{2}},$$

where a_s is between 0.81 and 1.04 for $Z \in [50, 100]$. As dimensions change, Z could become as high as 400, for which a_s is between 0.81 and 0.91. For either case, the lower value of 0.81 is taken to be conservative.

The number of circumferential waves present in buckling is

$$N = \pi(1-\nu^2) b_s \left(\frac{a}{L}\right)^{1/2} \left(\frac{a}{t}\right)^{1/4},$$

where b_s is between 0.8 to 1.15 for the range of Z values.

This value gives between 3 and 5 waves depending on material/dimensions. Donnell's shell theory will only give errors of $\sim 4\%$ at 3 waves. Above 3 waves the error decreases quickly. For graphite at current dimensions we have 5 waves, assuring accuracy.

To get critical load (P_c), set $\tau_f = \tau_b$ and solve for P :

$$P_c^s = \frac{\pi^3 E}{12(1-\nu^2)^{\frac{5}{8}} a_s} \frac{a^{1/4} t^{9/4}}{L^{1/2}}$$

Bending Instability

Bending instability can also occur in the case of transverse loading. This will occur as local buckling when the maximum stress (tensile or compressive) is exceeded. Approximating the tube as a membrane, the stress is $\sigma_b = PL/a^2 t \pi$. The tube fails at a critical stress reasonably approximated by

$$\sigma_c = \frac{E}{\sqrt{3(1-\nu^2)}} \frac{t}{a}.$$

Combining these gives the critical load for localized bending buckling as:

$$P_c^b = \frac{E \pi}{\sqrt{3(1-\nu^2)}} \frac{t^2 a}{L}$$

Material Failure: Normal Stresses

The material may fail simply from exceeding its normal stress limit, σ_f where σ_f is the minimum of tensile or compressive strength. Then the failure load for this failure is:

$$P_c^{mb} = \sigma_f \pi \frac{a^2 t}{L}$$

Material Failure: Shear Stresses

Failure can also occur from the tube exceeding its shear stress limit, τ_f . In ductile materials, $\tau_f \approx \sigma_f/2$ or $\sigma_f/\sqrt{3}$. Brittle material values (such as graphite) can be approximated from $\tau_f = \sigma_t \sqrt{R/3}$ where $R = \sigma_c/\sigma_t$ (compressive/tensile).

Given τ_f , the predicted critical load for shear failure is:

$$P_c^{ms} = \tau_f \pi at$$

Plotting Failure Curves

Using the available material properties, we are able to produce the following graphs in figure 2. Each point along each line represents the radius and thickness that will give a failure load of 145lbs (as found in Dennis' tower break test). The upper right side of each line represents safe design dimensions. The green line follows the dominating failure mode at any point along the graph, therefore, the dimension space above this line represents safe design space.

The predicted failure curves for CDMS graphite can be seen in the upper-left graph. The predicted dimensions for CDMS Graphite deviate 15 – 23% from actual values of Radius = 1in, Thickness = 0.028in. The graphite model is still rough, however, as the values of tensile and compressive strength used were those approximated in table 3. These should be verified before further progress is made.

2.3.5 Minimizing Radioactivity and Heat Load

Once the optimal dimension pairs (radius, thickness) are obtained along the failure limit, we can minimize radioactivity and heat load of the candidate materials. Radioactivity is directly proportional to volume, and thermal power is directly related to cross-sectional area. Holding tube lengths fixed, minimization of radioactivity and heat load is reduced to the problem of minimizing cross-section. Therefore, radioactivity and heat load will have identical minimization parameters.

The graphs in figure 3 plot radioactivity and thermal power as a function of radius. The thickness of the tube at any radius is implicitly the thickness from the optimal dimension pairs obtained from the failure limit lines in figure 2.

It is obvious that the candidate materials offer significant improvement over the current UF-4S Graphite. The heat load improvement per stage is examined below. For simplicity, the values along the optimum lines have been used.

5K -1K

At a radius of 0.4 inches, the power from Vespel SP-1 is $50\mu\text{W}$. This is 1/6 the current heat load. Assuming the same thermal conductivity for Vespel SCP-5000, this number could be reduced to near $35\mu\text{W}$ for more than an 800% reduction in heat load.

1K-100mK

Vespel SP-1 could reduce the heat load to $1.3\mu\text{W}$ from $3.4\mu\text{W}$, 2.6 times less than the current heat load. Vespel SCP-5000 could offer an additional 30% improvement over SP-1.

100mK-40mK

With no data yet in this range for Ti 15-3-3-3 we cannot know the improvement, but at the optimum value, cross-section is reduced by nearly a factor of 20. Given that the thermal conductivity of Ti 15-3-3-3 is almost certainly lower at this stage than UF-4S Graphite, a significant improvement is expected.

For each stage, the candidate materials not only offer a significant reduction in thermal power, but remain well within acceptable limits for radioactivity.

It should be noted that the optimized values would almost certainly result in a failure load of less than 145lbs. Given the error for the predicted Graphite failure, the actual would be around 20-30% lower. Even so, our failure load would still be near 100lbs. If it is decided that this is too low, the material dimensions can easily be increased and still offer more than a factor of 2 improvement for each stage.

2.4 Striplines

In addition to modifying the tower support tubes, we are examining the feasibility of replacing the NbTi vacuum coaxial cables along tower face with a parallel strip transmission line. This transmission line must satisfy the new inductance requirements of

the SQUID/Detector designs while remaining within acceptable limits for thermal power loading on the tower stages. Critical current density, resistivity, and critical temperature (T_c) must also be evaluated for the new line.

Our consideration of a flex cable comes from:

- Low inductance design capability
- Precise control over dimensions
- Reproducibility
- Strength, and Low Radioactivity (from Kapton substrate)

The new SQUID design will reduce the superconducting QET resistance from 0.2Ω to 0.02Ω . Since the 3dB roll-off frequency corresponds to R/L for our amplifier, when we reduce R by a factor of 10, we must also reduce inductance, L, by a factor of 10 to maintain our bandwidth. The new goal for the inductance of our flex cable is 30nH over a 20 inch length, or $\approx 60\text{nH/m}$. To determine the inductance for our parallel traces we used the following formula used by basic inductance calculators:

$$L \approx \frac{\mu_0 \mu_r h}{w} \quad (h > t, w \gg h)$$

μ_0 = the magnetic constant ($4\pi \cdot 10^{-7}$)

μ_r = relative permeability of Kapton (assumed to be 1)

t = thickness of trace

h = center-to-center separation of traces

w = width of the trace

Sonnet EM modeling software will be used to provide more detailed inductance modeling as well as to measure electrical cross-talk.

2.4.1 NbTi Trace

We have ordered Nb47Ti(53% Nb, 47% Ti by weight) which was rolled by Virginia Fine Metal. The foil is 4" x 10" and 0.002" thick.

The same Nb47Ti has already been successfully etched so it can now be made into a preliminary parallel strip transmission line for testing.

2.4.2 Ti 15-3-3-3 Trace

Ti 15-3-3-3 is another option as a trace material. Its relevant properties are discussed below.

- Thermal Conductivity: This alloy offers a lower thermal conductivity than NbTi at all stages.
- Critical Current Density: MUST EXPERIMENTALLY DETERMINE
- Superconducting Transition Temperature: 3.89K
- Resistivity: MUST EXPERIMENTALLY DETERMINE

Due to its very low transition temperature, it is not an option at the 4K to 600mK transition. If the SQUIDS are placed at the 600mK stage, Ti 15-3-3-3 is an ideal choice as a trace from 600mK down to the 10mK base.

To roll Ti 15-3-3-3 we have contacted Ulbrich, a company which could provide us with a foil as thin as 0.5 mil. The cost for even 1 mil, however, is \$1010/lb with a minimum of 10 lbs, so it will be expensive. Another possible company is called Arnold Rolled Products. They carry Ti 15-3-3-3 sheet in stock and could roll to 0.5 mil.

2.4.3 New 50mK Stage (or 100mK for Non-Ideal) Heatsink

The current tower design has an internal heat sink for the 50mK stage. The only external components of this stage on the tower face are two connectors for thermally connecting the tower support tubes to the fridge.

This new transmission line design, while easily adjustable to meet inductance requirements, is much more thermally conductive; therefore, to implement this new design, I propose adding an additional external component for heatsinking the transmission line to the 50mK fridge stage. The need for an external 50mK heatsink can be seen in Table 5. We have used a best case transmission line design: 0.5 mil Ti 15-3-3-3 designed for 50nH/20". This is compared to the current NbTi vacuum coax's and graphite tower support tubes. The power shown is per tower with the current 6-sided design.

Assuming the internal 50mK stage heatsink can be brought out, we can have a thermally competitive design for the parallel strip transmission line. Table 4 compares an NbTi line, Ti 15-3-3-3 line, current coax's, and the Graphite tube. NbTi only goes to 1 mil, as it cannot be rolled thinner. Ti 15-3-3-3 is presented in 0.5 mil and 1 mil, as it can be produced in 0.5 mil, but it will be expensive.

2.5 Availability

2.5.1 Vespel SP-1/Vespel SCP-5000

Vespel SP-1 and SCP-5000 are both readily available from DuPont through the certified distributor Curbell Plastics.

As a warning, an employee from Curbell Plastics notified us that another company, Pro Plastics, sells a counterfeit material under the name of Vespel.

2.5.2 Carbone UF-4S

This is the grade currently used in the towers as a support tube. Through recent contact with Mersen (the new owner of Carbone of America) we have found that this grade is still produced and readily available.

2.5.3 Ti 15-3-3-3/Ti 21s

Ti 15-3-3-3 is not available in anything except sheet form in the United States. Chinese companies, however, have Ti 15-3-3-3 available as wire, sheet, and rod. Two possible companies are YR Titanium and ReTi Metal. Two rods have been ordered from ReTi Metal.

Ti 21s is another metastable- β alloy with similar properties to Ti 15-3-3-3. Tests will be conducted to determine its suitability.

2.5.4 Stripline Companies

Rolling

- Hamilton Materials
- Virginia Fine Metals
- Arnold Rolled Products

Transmission Line Fabrication

- Luxel
- Tech-Etch

2.6 Appendix A: Aluminum as a Candidate Trace Material

Aluminum is naturally under consideration as a trace material, due to its well known properties and widespread use. Fabrication time for a stripline would be reduced by using Aluminum, as the company fabricating the line, Tech-Etch, has used it as a trace material in the past. A new material, such as Ti15-3-3 would require significantly more time to go through the development process. Therefore, it is in our best interest to examine the feasibility of an Aluminum-trace stripline. Considerations for its suitability include its thermal conductivity, coefficient of thermal expansion (CTE), and critical temperature (T_c).

2.6.1 Thermal Conductivity of Al5056

The Aluminum used by Tech-Etch is 5052-H19, however members of our collaboration were unable to find low temperature thermal conductivity data for this alloy. The thermal conductivity of another alloy, Al5056, was found to be very similar in normal state, so was used a proxy for 5052-H19. The thermal conductivity of Al5056 was determined from [?] for the range 600mK down to 50mK as,

$$K(T) = 1.9 \cdot 10^4 T^{2.83} \mu W/cmK \quad (2.5)$$

This thermal conductivity is compared to other phonon stripline candidate materials in Figure 4 below. In the range of interest (600mK - 50mK) we can see that the thermal conductivity of Al5056 is almost two orders of magnitude higher than NbTi and Ti15-3-3.

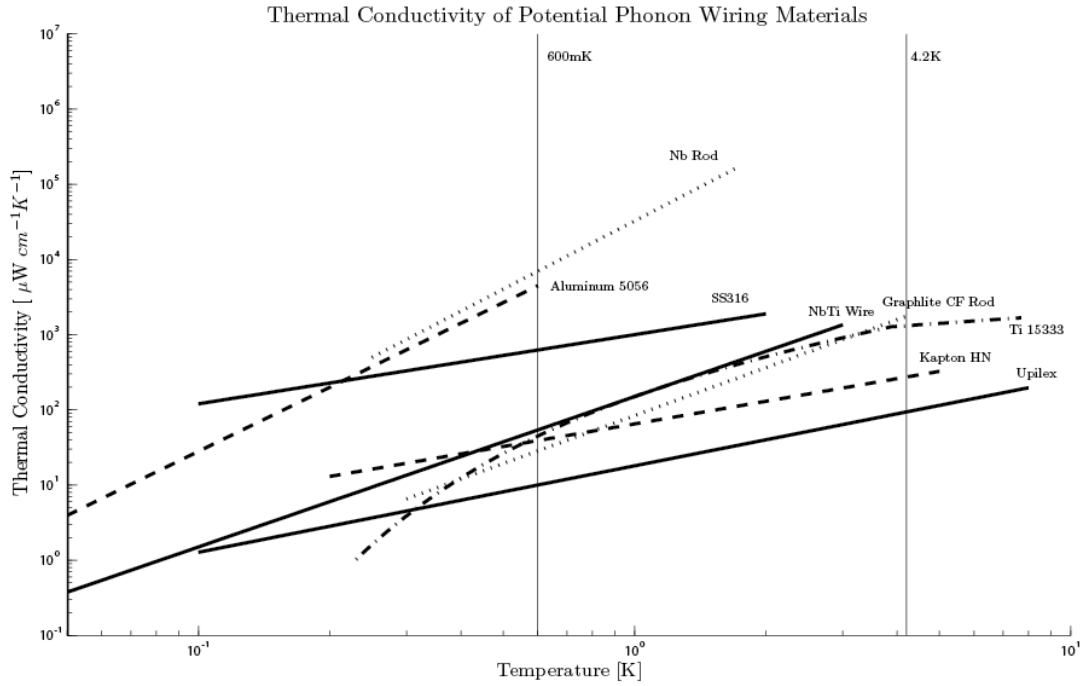


Figure 2.2: Thermal conductivities of various stripline candidate materials. The thermal conductivity of Al5056 is nearly two orders of magnitude higher than NbTi or Ti15-3-3

2.6.2 Aluminum Heat Load

To see if Al will work as a trace material, the thermal power conducted from 600mK to 50mK must be within our thermal budget for the 50mK still of our fridge. The power conducted between a thermal gradient is given by equation 1 in the report. Using a thickness of 1 mil, width of 40 mils, and a trace length of 0.79 inches we can calculate the power for each trace. Assuming 16 traces per detector and 6 detectors per tower,

Material	Power/Trace [nW]	Total Load per Tower [nW]
Ti 15-3-3-3	0.85	684
NbTi	1.4	739
Aluminum	92	9471

Table 2.7: Estimated heat load for an Aluminum-trace flex cable from 600mK to 50mK as compared with other candidate materials. Assumes 1 mil thick, 40 mils wide, 0.79 inch long traces; 16 traces per detector and 6 detectors per tower.

as well as accounting for Kapton heat load, we are able to estimate the total flex cable heat load per tower. The loads for Al5056 are compared with other trace materials in table 7.

The thermal budget for the 50mK end (the still) is $\sim 1\mu W$. The Al5056 trace heat load is an estimated $9.5\mu W$ per tower. The heat load for one tower is higher than the thermal budget, though our experiment necessitates the use of multiple towers. Reducing the width of the traces, as well as lengthening the traces could reduce this to perhaps $1\mu W$ (still too high), but inductance constraints would significantly complicate the design.

2.7 Thermal Expansion Coefficient of Aluminum

It is important to match the expansion coefficients of materials which will undergo large temperature changes. In our flex cable, we will be epoxy-ing the Aluminum traces to Kapton polyimide, so the CTE of these two materials should match relatively well. The linear coefficient of thermal expansion presented for Aluminum is 24ppm/K while DuPont states the coefficient for Kapton HN to be 20ppm/K. These values are well matched, so in this regard, Aluminum suites our needs.

2.8 Critical Temperature

The trace material for our striplines must be in a superconducting state for the temperatures at which they are used. The alloy used by Tech-Etch, 5052-H19, has a T_c of 775mK. This low T_c limits the alloy's use to the 600mK - 50mK span of our flex cable, as it would be in a normal state for most of the 4.2K - 600mK span. The low T_c of the alloy is a concern, due to non-ideal temperatures in our fridge. If the temperature drifts upward past the T_c of the Aluminum, then the traces will transition to a normal state. Fridge temperatures have been to drift up to as much as 1K, so this is a serious concern for the feasibility of an Aluminum-trace stripline.

2.9 Conclusion

Due to the high thermal conductivity of Aluminum, and the resulting heat load, as well as the low T_c , our collaboration has decided that it is unsuitable as a trace material.

Bibliography